

## Article

# Identification of Key Factors Influencing Sound Insulation Performance of High-Speed Train Composite Floor Based on Machine Learning

Ruiqian Wang <sup>1,2</sup>, Dan Yao <sup>3</sup>, Jie Zhang <sup>4,\*</sup> , Xinbiao Xiao <sup>1</sup> and Ziyang Xu <sup>2</sup><sup>1</sup> State Key Laboratory of Traction Power, Southwest Jiaotong University, Chengdu 610031, China<sup>2</sup> School of Mechanical Engineering and Rail Transit, Changzhou University, Changzhou 213164, China<sup>3</sup> Aviation Engineering Institute, Civil Aviation Flight University of China, Guanghan 618307, China<sup>4</sup> State Key Laboratory of Polymer Materials Engineering/Polymer Research Institute, Sichuan University, Chengdu 610065, China

\* Correspondence: zh.receive@gmail.com

**Abstract:** The body of a high-speed train is a composite structure composed of different materials and structures. This makes the design of a noise-reduction scheme for a car body very complex. Therefore, it is important to clarify the key factors influencing sound insulation in the composite structure of a car body. This study uses machine learning to evaluate the key factors influencing the sound insulation performance of the composite floor of a high-speed train. First, a comprehensive feature database is constructed using sound insulation test results from a large number of samples obtained from laboratory acoustic measurements. Subsequently, a machine learning model for predicting the sound insulation of a composite floor is developed based on the random forest method. The model is used to analyze the sound insulation contributions of different materials and structures to the composite floor. Finally, the key factors influencing the sound insulation performance of composite floors are identified. The results indicate that, when all material characteristics are considered, the sound insulation and surface density of the aluminum profiles and the sound insulation of the interior panels are the three most important factors affecting the sound insulation of the composite floor. Their contributions are 8.5%, 7.3%, and 6.9%, respectively. If only the influence of the core material is considered, the sound insulation contribution of layer 1 exceeds 15% in most frequency bands, particularly at 250 and 500 Hz. The damping slurry contributed to 20% of the total sound insulation above 1000 Hz. The results of this study can provide a reference for the acoustic design of composite structures.

**Keywords:** high-speed train; composite structure; sound insulation; key factor identification; machine learning; contribution analysis



**Citation:** Wang, R.; Yao, D.; Zhang, J.; Xiao, X.; Xu, Z. Identification of Key Factors Influencing Sound Insulation Performance of High-Speed Train Composite Floor Based on Machine Learning. *Acoustics* **2024**, *6*, 1–17. <https://doi.org/10.3390/acoustics6010001>

Academic Editor: John Kennedy

Received: 12 November 2023

Revised: 7 December 2023

Accepted: 15 December 2023

Published: 20 December 2023



**Copyright:** © 2023 by the authors. Licensee MDPI, Basel, Switzerland. This article is an open access article distributed under the terms and conditions of the Creative Commons Attribution (CC BY) license (<https://creativecommons.org/licenses/by/4.0/>).

## 1. Introduction

Improving the sound insulation performance of the car body structure of high-speed trains is a crucial step in controlling interior noise [1,2]. However, these train bodies consist of complex composite structures with multiple material layers of various classes. The sound insulation performance is highly dependent on the physical properties of each material [3,4]; hence, optimizing the sound insulation design of a high-speed train composite structure is very difficult.

As shown in Figure 1, the composite structure of the floor primarily includes the floor cloth, inner floor, support body (wood bone and elastic support), multiple material layers (sound insulation material, sound absorption material, damping material, and draining board), and corrugated aluminum profiles. For many component materials, researchers are concerned about the layer of materials that should be adjusted and how the layer should be adjusted to efficiently and accurately obtain the optimal solution to meet the requirements

of sound insulation. To achieve this goal, it is necessary to first fully determine the materials that have an impact on the overall sound insulation performance of the structure as well as the level of impact. This could help researchers to accurately identify and grasp the key factors affecting sound insulation and obtain a targeted adjustment and improvement of the materials with greater impact.

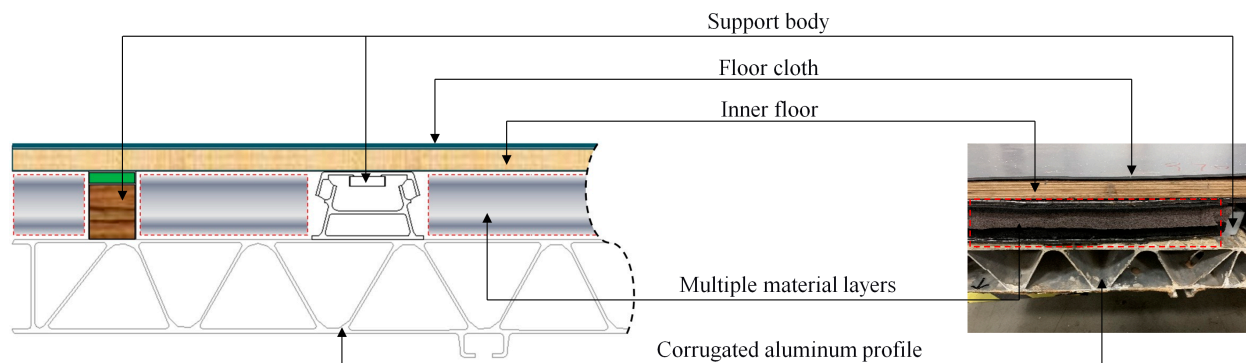


**Figure 1.** Cross-section of a typical high-speed train floor structure.

In previous studies, research on the factors influencing the sound insulation of the composite floor structure of high-speed trains tended to use simulation analysis methods. Zhang et al. [5] proposed a detailed equivalent modeling process for the full-size floor structure of a high-speed train based on the finite element method and statistical energy analysis method; they evaluated the influence of the floor cloth, built-in plate, aluminum profile, support body, and sandwich material on the overall sound insulation characteristics. Zheng et al. [6] analyzed the sound transmission loss of aluminum profiles in high-speed trains by using the structure–acoustic coupling finite element method; they investigated the effects of the total thickness of the plates and both the angle and thickness of the ribs on the sound transmission loss of the profile. Lin et al. [7] evaluated the influence of acoustic bridges, plate thickness, and structural materials on the acoustic and vibration performance of aluminum profiles, performed an optimization design, and established a structure with better acoustic and vibration performance. Based on the 2.5D FE-BE vibration acoustic model, Deng et al. [8] evaluated the effects of core porous materials and supports on the overall sound insulation performance of a floor composite structure. Yao et al. [9] evaluated the influence of the damping layer area on the acoustic and vibration performances of a train floor, effectively improving the acoustic and vibration performances of middle- and low-frequency floor structures. Wang et al. [10] evaluated the influence of the laying sequence of the core layer insulation and sound-absorbing materials on the sound insulation characteristics of the composite floor structure of a high-speed train and proposed the laying strategy of the core layer materials for the “centralization of sound absorbing materials in the middle and clamping sides of sound insulation materials”, which effectively improved the sound insulation characteristics at medium frequencies. Kim et al. [11] applied coupled-waveguide finite element and boundary element methods to predict the radiation efficiency and acoustic transmission of aluminum profiles for train compartment floors, taking into account the acoustic cavity.

The above research results provide an important theoretical basis and data support for guiding the sound insulation optimization design of composite floor structures of high-speed trains. However, these studies are essentially single-parameter investigations of one or several materials and do not consider the multi-parameter changes and influences among all the materials that constitute the floor composite structure. Moreover, it is difficult to comprehensively determine the degree of influence of each material using traditional simulation analysis methods. It is urgent to calculate the contribution of each material layer to the overall sound insulation of the composite floor structure based on a new method

and further identify one or more key factors with the most significant impact on the overall sound insulation performance through sequencing.

Owing to the rapid development of artificial intelligence, machine learning has been successfully applied as a core technology in numerous fields, such as pattern recognition, feature classification, data mining, and model prediction [12]. In the importance assessment and identification of the influencing factors, machine learning provides a variety of effective methods. Ahmad et al. [13] used principal component analysis to extract the features that best represented the working state of multistage centrifugal pumps and proposed a fault diagnosis method with high accuracy. Rahman et al. [14] proposed a fault diagnosis model based on the random forest algorithm, which accurately identified power transformer faults through dissolved gas analysis and was superior to traditional diagnostic methods in terms of classification accuracy and efficiency. Zhou et al. [15] proposed a fault isolation method based on the k-nearest neighbor rules to identify the fault causes of industrial processes with nonlinear, multimode, and non-Gaussian distributed data, which could isolate multiple sensor faults under relatively loose conditions. Casaburo et al. [16] applied a Gaussian machine-learning algorithm to the structural design and characterization of porous acoustic metamaterials and achieved good results. Eddin et al. [17] used an artificial neural network method to evaluate the influence of materials, thickness, density, size, and quality of light wood flooring on sound insulation, and the prediction error of 250~1000 Hz was no more than 2 dB. Aloisio et al. [18] built classification models based on multinomial logistic regression (MLR) and artificial neural networks (ANNs); they calibrated seismic data that were theoretically less affected by personal bias. Malekjafarian et al. [19] proposed an artificial neural network (ANN) algorithm to deal with the acceleration response energy of trains, using the acceleration response measured on trains in service to detect the stiffness loss of track sublayers.

In this study, a machine learning model for evaluating the importance of the sound insulation features of a composite floor structure was established based on the random forest method. The contribution of each material in the composite floor structure of a high-speed train to the overall sound insulation was comprehensively calculated and analyzed, and the key factors influencing its sound insulation performance were identified. In Section 2, we introduce the sample acquisition and material composition of the floor composite structure, stratify the structure according to the spatial position of the materials, and construct a feature database. In Section 3, a model for the feature contribution calculation based on random forest is established. In Section 4, the contribution of each material to the overall weighted sound insulation index is analyzed, and the influence of each material of the core layer on the overall sound insulation performance at different frequencies is analyzed to clarify the key influencing factors and optimization direction of sound insulation. Finally, the conclusions are presented in Section 5.

## 2. Machine Learning Method, Sound Insulation Prediction, and Optimized Design Flow of Composite Structure

### 2.1. Sound Insulation Test

The sound insulation samples were all tested and obtained based on the double reverberant chamber method [20]. As shown in Figure 2, the source and receiver chambers were separated by an acoustic wall, and their volumes were 73.3 m<sup>3</sup> and 61.7 m<sup>3</sup>, respectively. Six microphones were arranged on their floors, and the technical inspection of the number and position of loudspeakers and microphones was completed before the test. The size of the test specimen was 985 mm × 970 mm. During the test, the specimen was installed in the acoustic isolation hole and the periphery was well sealed with oil slurry. A white noise sound field was applied in the source room using a non-directional loudspeaker, and the average sound pressure levels  $L_1$  and  $L_2$  of the two chambers were tested simultaneously in the source chamber and the receiving chamber at a frequency of 100 Hz~5000 Hz. Then, the sound insulation of the tested specimen can be obtained by Equation (1).

$$R = L_1 - l_2 + 10 \lg \frac{ST}{0.161V} \quad (1)$$

where  $S$  is the surface area of the sample,  $T$  is the reverberation time of the receiving chamber, and  $V$  is the volume of the receiving chamber.

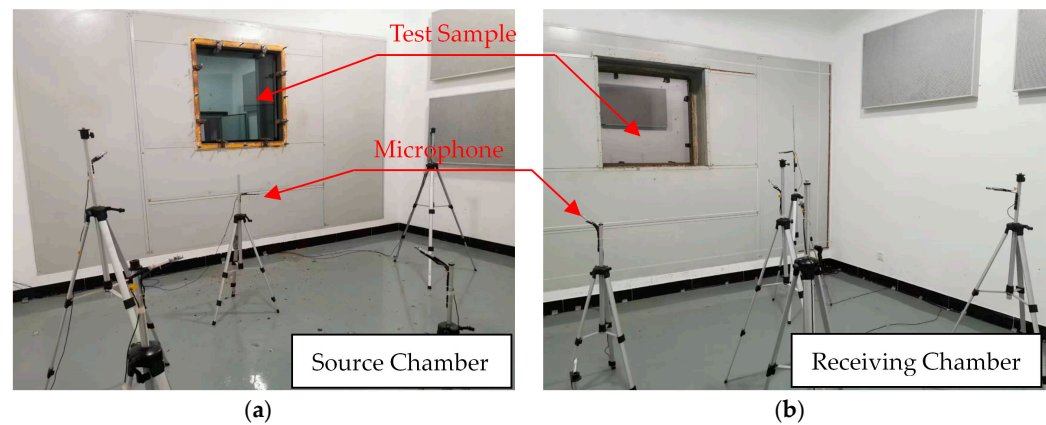


**Figure 2.** Sound insulation test site based on double reverberation chamber method. (a) Source chamber; (b) Receiving chamber.

The floor of a high-speed train is a multi-material composite structure that needs to be assembled using various types of materials, as shown in Figure 1. For each floor structure assembly, sound insulation tests are carried out according to a single process and the sound insulation results are obtained.

## 2.2. Initial Sample Set

Benefiting from the accumulation of acoustic insulation data for a large number of high-speed train floor composite structures, this study directly constructs an initial sample set based on experimental data. There were 118 datasets in the initial sample set. The basic structure of each test sample was approximately the same (Figure 1); however, the material compositions differed. Consider the material group of three typical floor structure test samples as an example, as listed in Table 1.

**Table 1.** Material composition and structure stratification of the initial sample set.

No.	Sample #1	Sample #2	Sample #3
Floor cloth layer	Floor cloth #1	Floor cloth #2	Floor cloth #1
Inner floor layer	Inner floor #1	Inner floor #2	Inner floor #3
Sound-insulation layer #1	Soundproof felt #1	—	Soundproof felt #2
Sound-insulation layer #2	Soundproof felt #3	Soundproof felt #4	Soundproof felt #5
Sound-absorption layer #1	Sound-absorbing cotton #1	Sound-absorbing cotton #2	Sound-absorbing cotton #3
Sound-insulation layer #3	Soundproof felt #4	Sound-proof felt #3	—
Sound-absorption layer #2	—	—	Sound-absorbing cotton #2
Sound-absorption layer #3	Sound-absorbing cotton #4	Sound-absorbing cotton #5	Sound-absorbing cotton #6
Sound-insulation layer #4	Soundproof felt #5	Soundproof felt #2	Soundproof felt #6
Draining board layer	Draining board #1	Draining board #2	Draining board #2
Support body layer	Support body #1	Support body #2	Support body #2
Damping slurry layer	Damping slurry #1	—	Damping slurry #2
Aluminum profile layer	Aluminum profile #1	Aluminum profile #2	Aluminum profile #3

In Table 1, similar types of materials are placed in the same row as much as possible to perform structural stratification. After stratification by class, all the samples are divided into 13 structural layers, including one floor cloth layer, one inner floor layer, four sound-insulation layers, three sound-absorption layers, one draining board layer, one support body layer, one damping slurry layer, and one aluminum profile layer. When a particular material name, such as the inner floor is used, it is labeled as #1, #2, #3, etc., to show that at least one of the parameters of the material, for example its density or thickness, differs from other materials with the same name.

### 2.3. Construction of the Feature Database

Before calculating the contribution of sound insulation and identifying the key influencing factors, it is necessary to propose the factors that may affect the overall sound insulation characteristics of the composite floor structure as comprehensively as possible and organize these factors to form the original feature database. Based on the test results of the above 118 groups of samples and referring to previous research results [3,4], the following factors were considered as the original characteristics: (1) The surface density, thickness, and weighted sound insulation index ( $R_w$ ) [21] of each sound-insulation layer. In a floor composite structure, in addition to the sound-insulation layer composed of different types of sound-insulation felt, the floor cloth, inner floor, draining board, and aluminum profile layers should also be considered as sound-insulation layers. (2) The volume density, thickness, and noise reduction coefficient (NRC) [22] of each sound absorbing layer. (3) The height of the supporting body. (4) The thickness of the damping slurry layer.

In addition, owing to the requirements of the spatial assembly, the thicknesses of the floor cloth layer, inner floor layer, draining board layer, and aluminum profile layer were the same in all samples. Therefore, from the perspective of machine learning, these four thickness parameters have no impact on the results of regression and classification; they should be regarded as invalid features and removed before modeling.

Furthermore, in combination with the hierarchical order in Table 1, all variables listed as original features in the first two paragraphs of the analysis were numbered, thus forming 31 original features, as illustrated in Table 2. Table 2 further gives the sample size and value range of each feature.

**Table 2.** Original features of the floor structure.

Structure Layer Name	Feature Name	Feature No.	Sample Size	Value Range
Floor cloth layer	Surface density	F01	6	2–5 kg/m <sup>2</sup>
	$R_w$	F02	6	20–28 dB
Inner floor layer	Surface density	F03	8	8–16 kg/m <sup>2</sup>
	$R_w$	F04	8	27–36 dB
Sound-insulation layer #1	Surface density	F05	11	0.8–14 kg/m <sup>2</sup>
	Thickness	F06	8	1–7 mm
	$R_w$	F07	11	20–38 dB
Sound-insulation layer #2	Surface density	F08	9	2–8 kg/m <sup>2</sup>
	Thickness	F09	8	1.2–4 mm
	$R_w$	F10	9	22–32 dB
Sound-absorption layer #1	Volume density	F11	10	10–60 kg/m <sup>3</sup>
	Thickness	F12	13	10–40 mm
	NRC	F13	11	0.2–0.9

Table 2. Cont.

Structure Layer Name	Feature Name	Feature No.	Sample Size	Value Range
Sound-insulation layer #3	Surface density	F14	9	2–8 kg/m <sup>2</sup>
	Thickness	F15	8	1–4 mm
	$R_w$	F16	8	20–32 dB
Sound-absorption layer #2	Volume density	F17	9	10–60 kg/m <sup>3</sup>
	Thickness	F18	7	10–30 mm
	NRC	F19	7	0.2–0.7
Sound-absorption layer #3	Volume density	F20	10	10–24 kg/m <sup>3</sup>
	Thickness	F21	8	6–20 mm
	NRC	F22	7	0.2–0.6
Sound-insulation layer #4	Surface density	F23	10	2–10 kg/m <sup>2</sup>
	Thickness	F24	7	1–5 mm
	$R_w$	F25	10	20–35 dB
Draining board layer	Surface density	F26	5	0.1–0.5 kg/m <sup>2</sup>
	$R_w$	F27	5	6–12 dB
Support body layer	Height	F28	6	50–108 mm
Damping slurry layer	Thickness	F29	8	1–8 mm
Aluminum profile layer	Surface density	F30	6	32–40 kg/m <sup>2</sup>
	$R_w$	F31	6	33–41 dB

### 3. Feature Contribution Analysis Modeling Based on Random Forest

#### 3.1. Method Introduction

The sample number of the composite structure of the high-speed train floors involved in this paper is 118, which is not much. Moreover, the data is non-linear. Decision trees, random forests, support vector machines, etc., can be listed as alternative methods for machine learning regression modeling. However, random forest also has unique advantages. Random forest is a tree-based integrated machine learning algorithm [23,24]. It is a collection of many different types of random trees that can quickly process a large number of input variables at a low computational cost and shows excellent performance in classification and regression. To measure the importance of the sample features, random forest can quantitatively describe the degree of contribution of each feature to classification or regression [25–28], which is very suitable for the research object and purpose of this paper. Therefore, the random forest method is adopted in this paper.

The calculation of the feature contribution is realized synchronously in the process of regression analysis by the random forest method. The original characteristics are the surface density, thickness, and acoustic performance of each material layer, and the target variable is the overall sound insulation of the train floor structure. In other words, we use the constructed random forest model to carry out feature training and prediction of target variables. When each tree is trained, the importance of features can be calculated by observing the model's performance (Gini coefficient) on the data outside the bag.

As shown in Figure 3, the implementation process of the algorithm includes four steps: (1) Select  $n$  samples from the sample set as a training set using the method of sampling and placing back. (2) Generate a decision tree with the sample set obtained by sampling. At each generated node, randomly select  $d$  features without repetition and divide the sample set by  $d$  features to determine the best partition features. (3) Repeat steps (1) and (2) for a total of  $k$  times, where  $k$  is the number of decision trees in the random forest. (4) Use the

random forest obtained by training to predict the test sample and determine the predicted result by the voting method.

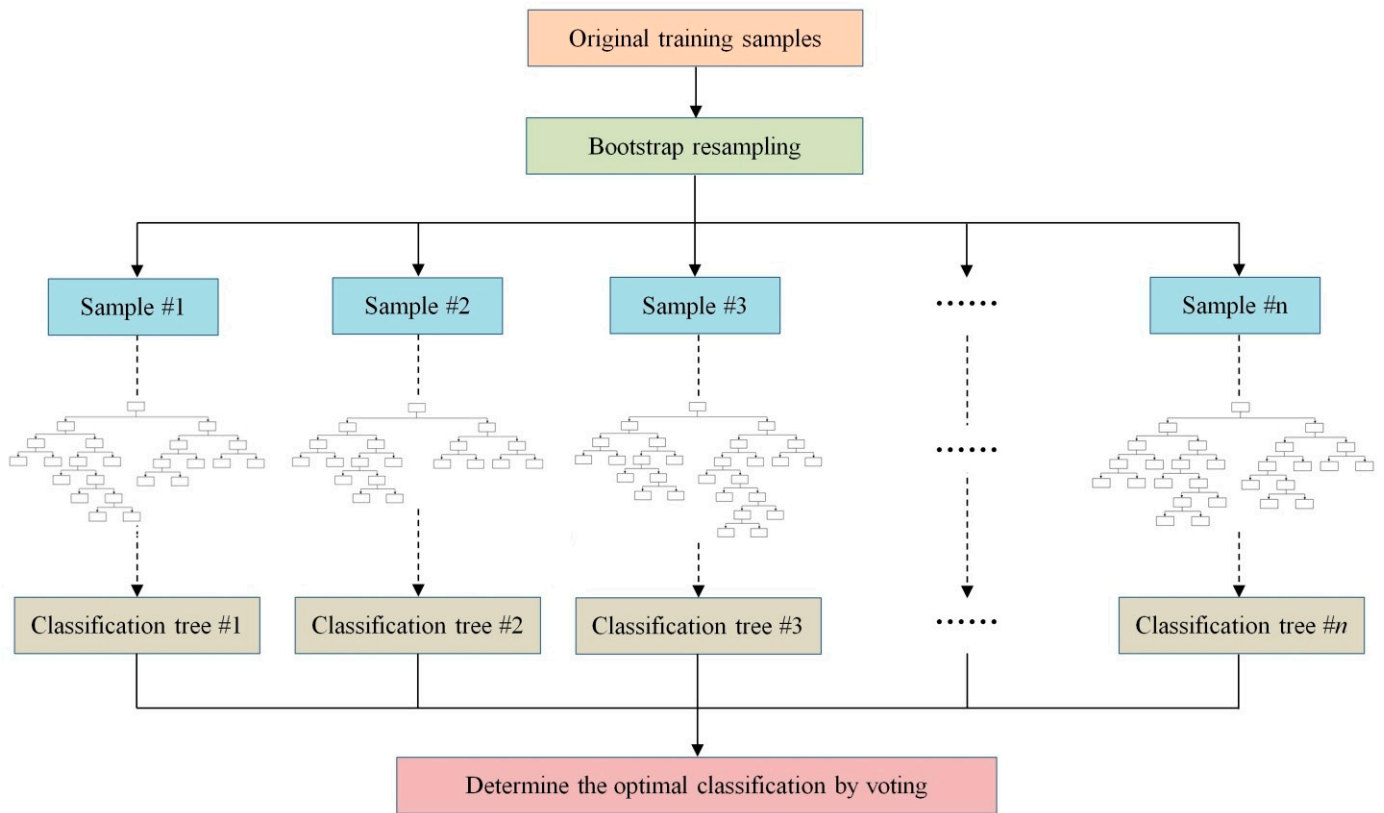


**Figure 3.** Flow diagram of the random forest algorithm.

In the random forest algorithm, the Gini index ( $GI$ ) is typically used as an evaluation index to measure the feature contribution ( $FC$ ) [23]. Considering the 31 features ( $F01, F02, F03, \dots, F31$ ) of the composite floor structure of the high-speed train in Table 2, it is assumed that there are  $I$  decision trees and  $C$  categories. This makes it necessary to calculate each feature of the  $GI$  score  $FC^{(Gini)}$ , that is, the average change of the  $j$ th feature in the node split impurity in all decision trees of the random forest.

The  $GI$  of node  $q$  in the  $i$ th tree can be obtained using the following formula:

$$GI_q^{(i)} = \sum_{c=1}^{|C|} \sum_{c' \neq c} p_{qc}^{(i)} p_{qc'}^{(i)} = 1 - \sum_{c=1}^{|C|} \left( p_{qc}^{(i)} \right)^2 \quad (2)$$

where  $C$  is the number of categories and  $p_{qc}$  represents the proportion of category  $C$  in node  $q$ ; that is, the probability that the two samples are randomly selected from node  $q$  and their category labels are inconsistent.

The contribution of the  $j$ th feature in node  $q$  of the  $i$ th tree, that is, the  $GI$  change before and after the node  $q$  branches, can be calculated using the following formula:

$$FC_{jq}^{(Gini)(i)} = GI_q^{(i)} - GI_l^{(i)} - GI_r^{(i)} \quad (3)$$

where  $GI_l^{(i)}$  and  $GI_r^{(i)}$  denote the  $GI$  of the two new nodes after branching. If the node where the  $j$ th feature appears in the  $i$ th decision tree is set  $Q$ , then the contribution of the  $j$ th feature in the  $i$ th tree is

$$FC_j^{(Gini)(i)} = \sum_{q \in Q} FC_{jq}^{(Gini)(i)} \quad (4)$$

Furthermore, because  $I$  trees exist in the random forest, the contribution score of each feature is

$$FC_j^{(Gini)} = \sum_{i=1}^I FC_j^{(Gini)(i)} \quad (5)$$

Finally, the contribution scores of all the features are normalized (the total score is equal to 1), which can be obtained as follows:

$$FC_j^{(Gini)} = \frac{FC_j^{(Gini)}}{\sum_{j'=1}^J FC_{j'}^{(Gini)}} \quad (6)$$

In addition, the value of hyperparameters in a random forest model may have a significant impact on the model performance. The hyperparameters mainly include the number of trees, the maximum depth of trees, the maximum number of features, the minimum number of samples required for leaf nodes, the minimum number of samples required for internal node splitting, and so on. Increasing the number of trees usually improves the performance of the model, but also increases the computational cost, and too many trees can lead to overfitting. Limiting the maximum depth of the tree can prevent overfitting, but too small a value can lead to too simple a model. A small maximum number of features can help prevent overfitting, but it is easy to increase the randomness of the model. The minimum number of samples required for leaf node and internal node splitting is often used to control tree growth, and larger values may result in a more conservative model.

The main hyperparameters in the random forest model are finally determined after searching within their respective value ranges by using an optimal algorithm. The final values of each parameter after tuning are shown in Table 3.

**Table 3.** The value of the hyperparameter in the model.

No.	Hyperparameter Name	Value
1	Number of trees	10
2	Maximum depth of the tree	9
3	Maximum number of features	6
4	Minimum number of samples required for leaf nodes	1
5	Minimum number of samples required for internal node splitting	4

Thus, a machine-learning model was established to evaluate the contribution of the sound insulation features of the composite floor structure of a high-speed train. According to the contribution size of each feature, all the features can be sorted from largest to smallest. The higher the ranking, the more significant the impact on the results and the more important it should be considered as a key influencing factor.

### 3.2. Generalization and Limitation Analysis of the Model

To verify the generalization ability of the model, 10-fold cross-validation was used. The data set was divided into 10 subsets; one subset was used as the validation set each time, and the rest were used as the test set. Ten groups of training and validation were performed on the model. Figure 4 gives the results of the cross-validation, still using  $MSE$  and  $R^2$  as the evaluation values. It can be seen that in the 10 groups of verification, the  $MSE$  of the training set and the test set are both below 0.015 and the  $R^2$  is above 0.88, indicating that the influence of different feature configurations on the model training results is within a controllable range. The model has good generalization.

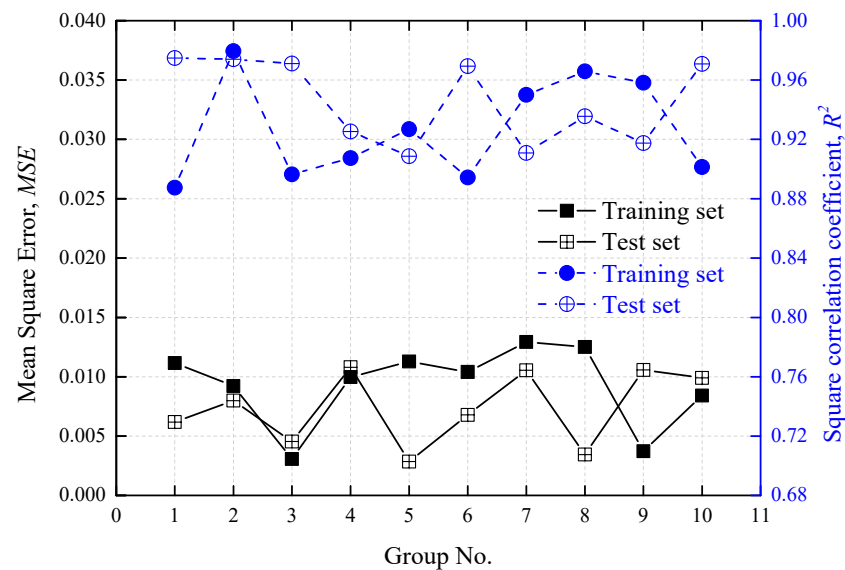


**Figure 4.** Cross validation results.

The limitations of random forest mainly include overfitting, inapplicability of high-dimensional sparse data, inapplicability of linear problems, poor predictive interpretation, sensitivity to noise, and so on.

The research object in this paper is the composite floor structure of high-speed trains, and the relationship between its characteristics and the target sound insulation quantity is nonlinear. In addition, in the process of acquiring experimental samples, the test personnel, test equipment, and test methods are always the same, and the test materials are well-preserved and well-processed, so that there is no very strange noise data in all the test results. Therefore, the overfitting, high-dimensional sparse data, and predictive interpretation are mainly explained.

(1) Overfitting. If the number of trees in the random forest is too large, it may cause overfitting training of the data. The database in this paper contains 118 groups of samples, so the effect of the number of trees varying between 5 and 15 on the model training results is investigated. Mean square error ( $MSE$ ) and square correlation coefficient ( $R^2$ ) were used as evaluation values. As shown in Figure 5, in general, when the number of trees varies between 5 and 15, the training results of the model are basically satisfactory. When the number of trees is 9 and 10, the  $MSE$  basically reaches its minimum, about 0.005. When the number of trees is 10,  $R^2$  reaches a maximum of about 0.98. Therefore, we set the number of trees in the model to 10, which is most suitable for the model.

(2) High-dimensional sparse data. For the sample data of the floor structure of the high-speed train in this paper, there are four sparse data, which are the thickness of the floor cloth layer, the thickness of the inner board layer, the thickness of the drain board layer and the thickness of the aluminum profile layer. They are the same in all samples. When processing high-dimensional sparse data, random forest may lose some information during feature selection, resulting in poor training effects. Therefore, in Section 2, they have been treated as invalid features and removed before modeling. For the remaining 31 features, each feature contains samples of no less than six values, as shown in Table 2, which will have a large or small impact on the training results and should be retained.

(3) Predictive interpretability. Random forests are often considered “black box” algorithms whose predictions are relatively difficult to interpret, especially for specific tree models. Therefore, it is often necessary to incorporate a SHAP plot to illustrate which features are most important and their range of influence on the data set. This will be shown in the subsequent analysis.

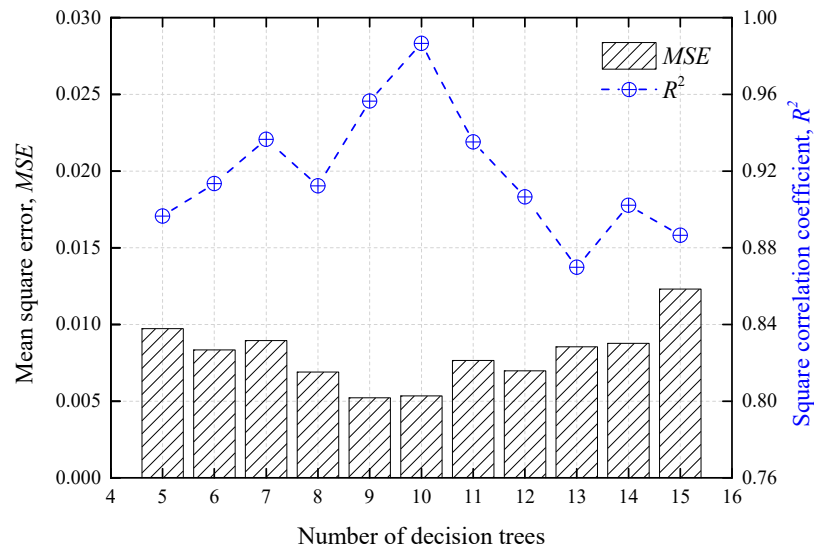


Figure 5. Influence of tree number change on model training results.

#### 4. Contribution Analysis and Identification of Key Influencing Factors

##### 4.1. $R_w$ Influencing Factors of the Entire Structure and Their FC Analysis

Figure 6 shows the calculation results for the contribution of each feature to the overall weighted sound insulation index, based on the random forest model. Further, Figure 7 shows the SHAP diagram of the model, which demonstrates the influence of various features on target variables more clearly by visualization. It can be seen that the results of Figures 6 and 7 are basically consistent, and the two verify each other.

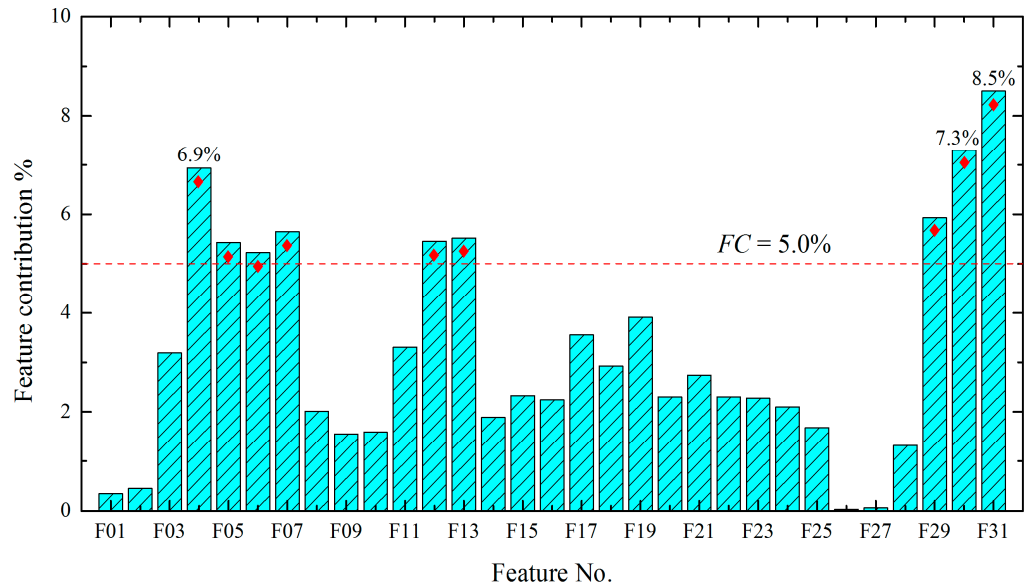
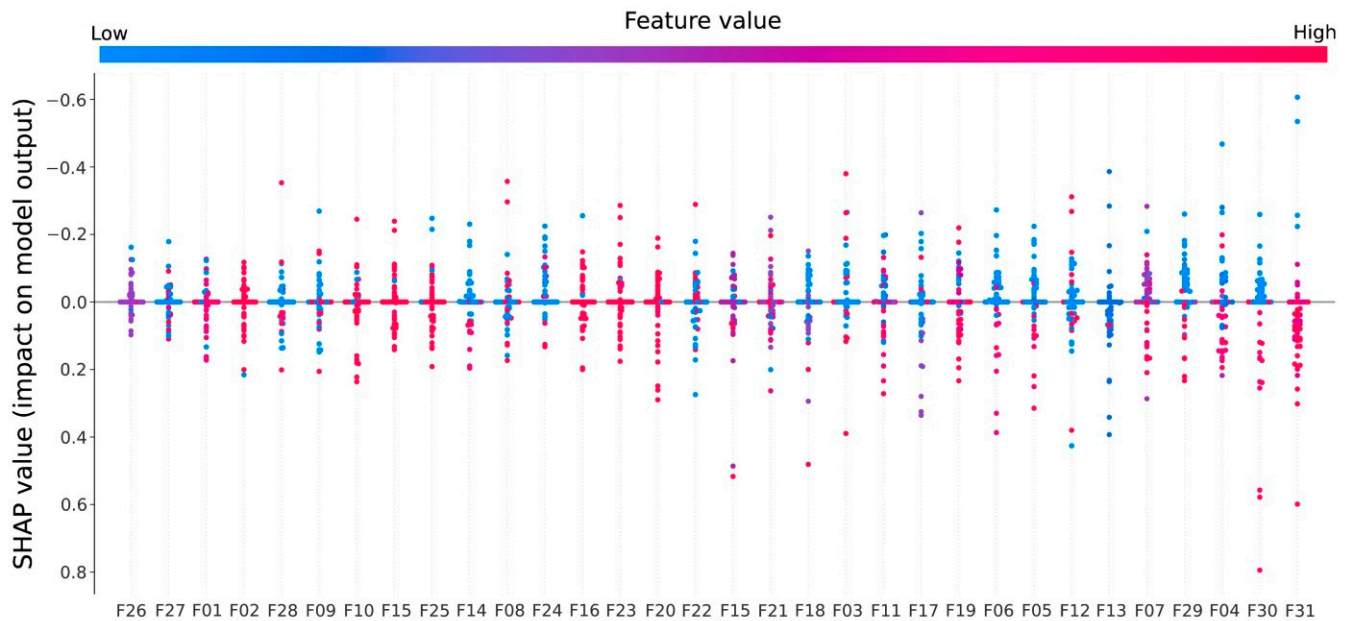


Figure 6. FC calculation results of each feature to  $R_w$  of the entire structure.

According to these requirements, several characteristics with the highest contribution can be selected as the key influencing factors. Here, we used the contribution  $FC = 5\%$  as the dividing line (red dashed line in Figure 6) to distinguish the key influencing factors. It can be observed that there are nine features that contribute more than 5%. The nine features were the identification results of the key factors affecting the sound insulation of the composite structure of the train floor.



**Figure 7.** SHAP diagram of the model.

Of these, the characteristics with the largest contributions were F31 and F30 (the weighted sound insulation index and the surface density of the aluminum profile layer), with contributions of 8.5% and 7.3%, respectively. This was followed by F04 (the weighted sound insulation index of the inner floor layer), with a contribution of 6.9%. This is consistent with the conclusions of previous studies [29,30]. This is because the aluminum profiles and internal panels are the two most important components of the composite floor structure, and their weight and thickness are the largest in the entire structure.

The other six features were located in the core layer and their contributions were between 5% and 6%. Among them, the contribution of F29 (the thickness of the damping paste layer) was 5.9%, which is the most influential factor after the aluminum profile and inner floor. This is because the damping slurry layer is directly laid on the inner surface of the aluminum profile; the thicker the layer, the more obvious the damping effect on the aluminum profile and the greater the impact on its sound insulation performance. In addition, it is worth noting that although the composite structure contains multiple sound insulation and absorption layers, only sound-insulation layer #1 and sound-absorption layer #1 have the greatest impact on the weighted sound insulation index of the entire structure.

In addition, in engineering design, owing to the structural strength, assembly space, and other constraints, the acoustic optimization design process of a high-speed train body is not random. Some key components are difficult to adjust, particularly the internal panels, aluminum profiles, and supports. Therefore, the measures of the acoustic optimization design are more concerned with the optimization of the core layer materials, such as the material selection and arrangement.

#### 4.2. FC Analysis of Acoustic Properties of Core Layer Materials to Sound Insulation at Different Frequencies

The weighted sound insulation index  $R_w$  of the structure was obtained from the measured frequency sound insulation curve after the weighted calculation [21]. Figure 8 shows the statistical results of the sound insulation values of the 118 sets of composite floor structure samples at each frequency in the range of 100–5000 Hz. It can be observed that the sound insulation value of each frequency has greater or smaller changes, and these differences affect the calculation results of  $R_w$ .

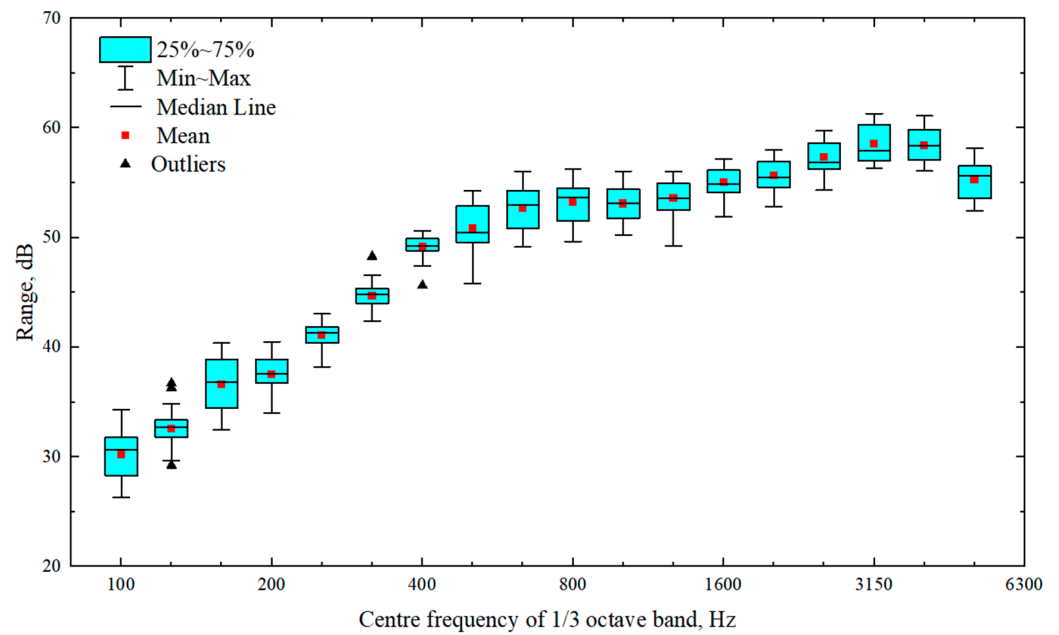


**Figure 8.** Statistical results of sound insulation values of each frequency.

To meet the  $R_w$  design requirements of the entire structure, it is necessary to carefully analyze the sound insulation value of the structure at each frequency, particularly to identify the frequency of the largest adverse deviation (weak link) to improve the sound insulation performance of these weak links. Figure 9 shows the measured sound insulation curves (blue curves) at different frequencies for samples #1 and #3 listed in Table 1. Simultaneously, by comparing the weighted sound insulation curve (red curve) with the measured curve, the weighted sound-insulation index  $R_w$  is calculated. It can be observed that for sample #1, the frequency bands of its adverse deviation (shadow region) are mainly 100–500 Hz and 1000–2000 Hz, and the maximum adverse deviation is 200–250 Hz. For sample #3, the frequency bands of its adverse deviation (shadow region) are 100–400 Hz and 800–1250 Hz, and the maximum adverse deviation is 100–125 Hz. Therefore, the weak frequency bands of sound insulation were not the same for different structural samples.

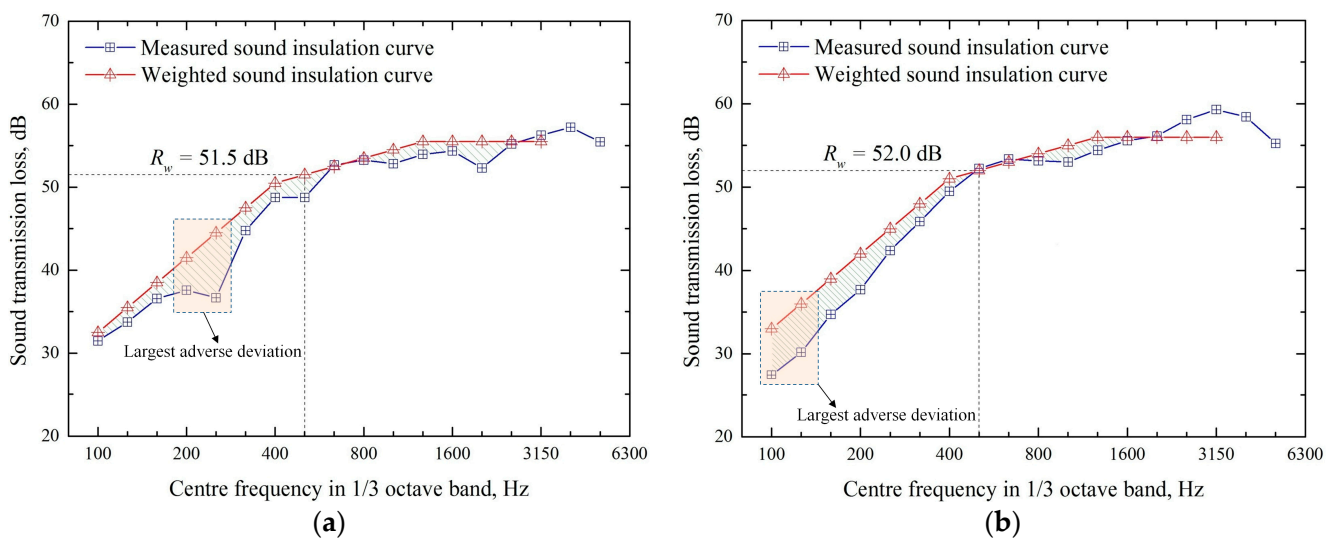


**Figure 9.** Measured sound insulation frequency curve of the structure and calculation of  $R_w$ . (a) Sample #1; (b) Sample #2.

Therefore, for frequency bands with weak sound insulation, researchers aim to determine the acoustic properties that play a leading role in the sound insulation of these frequency band, thus guiding researchers to propose targeted material optimization strategies.

Therefore, we can still calculate and analyze only the contribution of the acoustic properties of the core layer materials to the sound insulation of the structure at each frequency, according to the random forest model in Section 2. It is only necessary to extract the acoustic performance features related to the core layer material in Table 2 (the damping slurry layer only has a thickness feature; therefore, it is directly extracted) to form a new feature library. The original weighted sound insulation index and noise reduction coefficient were replaced with frequency-related sound insulation and sound absorption coefficients, as listed in Table 4.

**Table 4.** Sound insulation characteristics database of floor core materials.

Structure Layer Name	Feature Name	Original Feature No.	New Feature No.
Sound-insulation layer #1	Sound insulation value ( $f$ )	F09	FS01
Sound-insulation layer #2	Sound insulation value ( $f$ )	F12	FS02
Sound-absorption layer #1	Sound absorption coefficient ( $f$ )	F15	FS03
Sound-insulation layer #3	Sound insulation value ( $f$ )	F18	FS04
Sound-absorption layer #2	Sound absorption coefficient ( $f$ )	F21	FS05
Sound-absorption layer #3	Sound absorption coefficient ( $f$ )	F24	FS06
Sound-insulation layer #4	Sound insulation value ( $f$ )	F27	FS07
Draining board layer	Sound insulation value ( $f$ )	F30	FS08
Damping slurry layer	Thickness	F32	FS09

The sound insulation contribution of six octave center frequencies of 125–4000 Hz was calculated as an example, as shown in Figure 10a–f, clearly showing the influence of various core layer materials on sound insulation at different frequencies. The analysis was performed as follows.

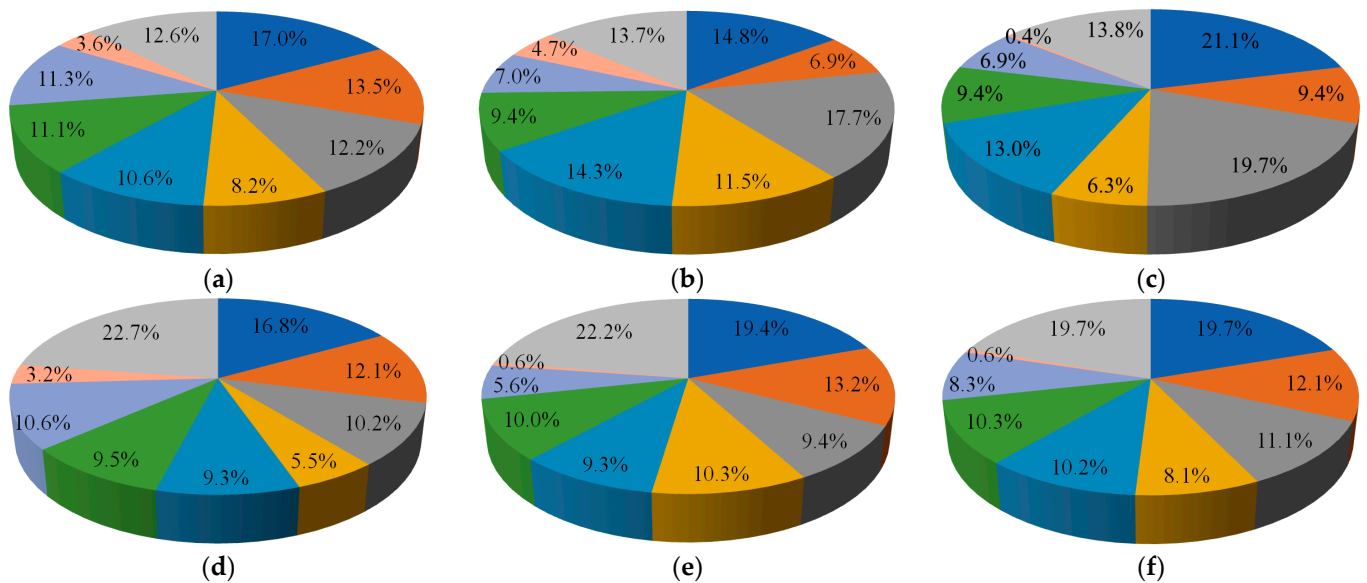


**Figure 10.** FC analysis results of acoustic properties of core layer materials to sound insulation at different frequencies. (a) 125 Hz; (b) 250 Hz; (c) 500 Hz; (d) 1000 Hz; (e) 2000 Hz; (f) 4000 Hz.

(1) The sound-insulation layer had a significant impact on the sound insulation of almost all frequency bands. The total contribution of the four sound-insulation layers was greater than 40% for each frequency band. In particular, sound-insulation layer #1 ranked among the top two in terms of the sound insulation contribution at various frequencies. Except at 250 Hz, the contributions exceeded 15% and reached 20%. This is related to the placement of sound-insulation layer #1 on the outermost side, which is the same mechanism as the relatively large contributions of the aluminum profile (including the damping paste) and inner floor.

(2) The sound-absorption layer has a significant impact on the middle- and low-frequency sound insulation, especially sound-absorption layer #1, which has a greater impact on the sound insulation at 250 Hz and 500 Hz, with a contribution of more than 15%. This is consistent with the conclusion in [10], mainly because the difference in the sound absorption coefficients of different sound absorption materials is concentrated in the intermediate frequencies.

(3) The sound insulation effect of the drain board layer on each frequency band is very small because the surface density of the several drain boards included in the layer is very small ( $0.1\text{--}0.5\text{ kg/m}^2$ ), the proportion of the entire composite structure is basically negligible, and the sound insulation value is also very low.

(4) The sound insulation contribution of the damping slurry layer to each frequency band is more than 10%, especially in the mid–high frequency bands above 1000 Hz, which is close to or even more than 20%. This is related to the greater impact of the mid–high frequency sound insulation on damping.

#### 4.3. Experimental Verification

As can be seen from Figure 11, the maximum adverse deviation positions of samples #1 and #3 are 250 Hz and 125 Hz, respectively. According to the calculation results in Figure 6, the sound insulation values of 250 Hz and 125 Hz are most affected by the feature FS03 (the sound absorption coefficient of sound-absorption layer #1) and FS01 (the sound insulation quantity of sound-insulation layer #1) respectively. Therefore, the following test verification conditions are set:

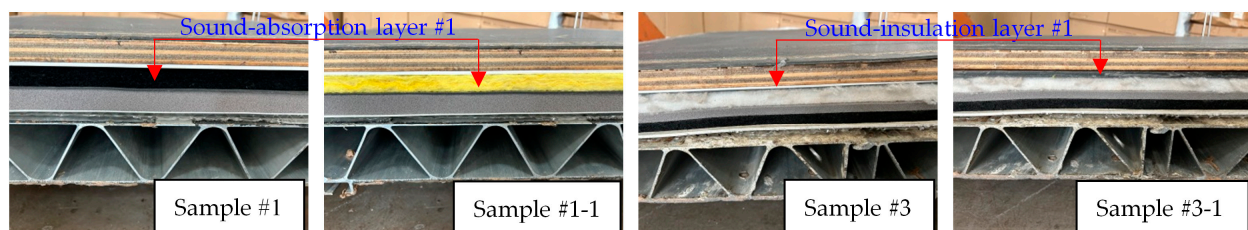


**Figure 11.** Cross sections of each test sample.

(1) The sound-absorption layer #1 of sample #1 was originally carbon fiber wool with a sound absorption coefficient of 0.55. During optimization, the material of the sound-absorption layer #1 was replaced with glass fiber wool, with a sound absorption coefficient of 0.70, to form the optimization scheme (sample #1-1) of sample #1.

(2) The sound-insulation layer #1 of sample #3 was originally a polyurethane sound insulation pad with a sound insulation capacity of 24 dB. During optimization, the material of sound-insulation layer #1 was replaced with a rubber sound insulation pad, with a sound insulation capacity of 36 dB, to form the optimization scheme (sample #3-1) of sample #3.

The test results are shown in Figure 12 below. As can be seen from Figure 12a, after sound-absorption layer #1 is replaced with a material with a higher sound absorption coefficient, the sound insulation value in most frequency bands is improved, and the improvement effect is most significant in the middle- and low-frequency bands. The sound insulation near 250 Hz is increased by nearly 3 dB, and the  $R_w$  of the whole floor structure is increased by 0.5 dB. As can be seen from Figure 12b, after sound-insulation layer #1 is

replaced with a material with higher sound insulation capacity, the sound insulation value in most frequency bands is improved, and the improvement effect is the most significant at 100–125 Hz and 500–800 Hz. The increase in these frequency bands is 1.5–2 dB, and the  $R_w$  of the whole floor structure is increased by 0.7 dB.

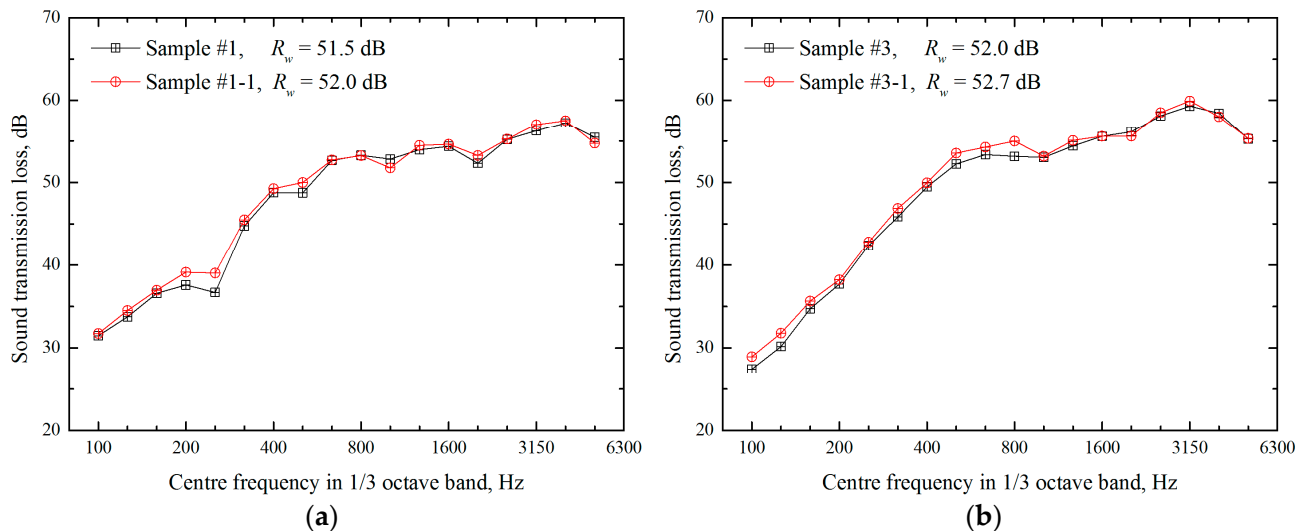


**Figure 12.** The result of sound insulation optimization verification. (a) Optimization validation of sample #1; (b) Optimization validation of sample #3.

The experimental verification results show that, according to the results in Figure 12, the sound insulation optimization of samples #1 and #3 has a good effect, thus verifying the correctness of the results in this paper.

In general, for the composite floor structure of high-speed trains, more attention should be paid to sound-insulation layer #1 and sound-absorption layer #1. The optimization of medium-frequency sound insulation should focus more on sound-insulation layer #1, sound-absorption layer #1, and the damping paste layer, whereas the optimization of high-frequency sound insulation should focus more on sound-insulation layer #1 and the damping slurry layer.

## 5. Conclusions

This study established a machine learning model for predicting the sound insulation of composite floors in high-speed trains based on data-driven analysis and identified the key factors affecting sound insulation. The following conclusions were drawn:

1. When all material characteristics were considered, the interior panel layer, sound-insulation layer #1, sound-absorption layer #1, damping slurry layer, and aluminum profile layer contributed the most to the sound insulation of the composite floor. The contributions of the sound insulation and surface density of the aluminum profiles and the sound insulation of the interior panels were 8.5%, 7.3%, and 6.9%, respectively.

2. Considering only the core layer material, each sound insulation material had a significant impact on the sound insulation of the composite floor in all frequency bands, particularly sound-insulation layer #1, whose sound insulation contribution exceeded 15% in most frequency bands. The sound-absorbing layer had a significant impact on the sound insulation at medium and low frequencies below 500 Hz, especially sound-absorbing material #1, which contributed more than 15% at 250 Hz and 500 Hz. The damping slurry layer had a significant effect on the high-frequency sound insulation above 1000 Hz, with a sound insulation contribution rate of 20%.

3. To optimize the sound insulation of the composite floor of a high-speed train for low-frequency bands (below 500 Hz), attention should be paid to sound-insulation layer 1# and sound-absorption layer 1#; for medium-frequency bands between 500 and 1000 Hz,

attention should be paid to sound-insulation layer 1#, sound-absorption layer 1#, and the damping slurry layer; and for high-frequency bands above 1000 Hz, attention should be paid to sound-insulation layer 1# and the damping slurry layer.

**Author Contributions:** R.W.: Conceptualization, Methodology, Resources, Data Curation, Writing—original draft. D.Y.: Methodology, Software, Writing—review and editing. J.Z.: Conceptualization, Methodology, Writing—review and editing. X.X.: Writing—review and editing. Z.X.: Writing—review and editing. All authors have read and agreed to the published version of the manuscript.

**Funding:** This research was funded by [National Natural Science Foundation of China] grant number [Nos. 52002257, U1934203], [Open Project of State Key Laboratory of Traction Power] grant number [No. TPL2205], [Changzhou Applied Basic Research Project] grant number [CJ20220020], the Natural Science Foundation of Sichuan Province (No. 2023NSFSC0902), and the Open Project of Key Laboratory of Flight Techniques and Flight Safety, CAAC (No. FZ2022KF01).

**Data Availability Statement:** The data used to support the findings of this study are available from the corresponding author upon request. The generated data and numeric model are not publicly available due to their critical role in another ongoing research projects.

**Conflicts of Interest:** The authors declare that they have no known competing financial interests or personal relationships that could have influenced the work reported in this paper.

## References

- Hardy, A.-E. Measurement and assessment of noise within passenger trains. *J. Sound Vib.* **2000**, *231*, 819–829. [\[CrossRef\]](#)
- Zhang, J.; Xiao, X.-B.; Sheng, X.-Z.; Zhang, C.-Y.; Wang, R.-Q.; Jin, X.-S. SEA and contribution analysis for interior noise of a high speed train. *Appl. Acoust.* **2016**, *112*, 158–170. [\[CrossRef\]](#)
- Wang, R.-Q.; Yao, D.; Zhang, J.; Xiao, X.-B.; Jin, X.-S. Sound-insulation prediction model and multi-parameter optimization design of the composite floor of a high-speed train based on machine learning. *Mech. Syst. Signal Process.* **2023**, *200*, 110631. [\[CrossRef\]](#)
- Arjunan, A.; Baroutaji, A.; Robinson, J. Perforated steel stud to improve the acoustic insulation of drywall partitions. *Acoustics* **2021**, *3*, 679–694. [\[CrossRef\]](#)
- Zhang, J.; Yao, D.; Wang, R.-Q.; Xiao, X.-B. Vibro-acoustic modelling of high-speed train composite floor and contribution analysis of its constituent materials. *Compos. Struct.* **2021**, *256*, 113049. [\[CrossRef\]](#)
- Zheng, X.; Ruan, P.-L.; Luo, L.; Qiu, Y.; Hao, Z.-Y. A numerical study on the sound transmission loss of HST aluminum extruded panel. *Noise Control Eng. J.* **2020**, *68*, 367–377. [\[CrossRef\]](#)
- Lin, L.-Z.; Ding, Z.-Y.; Zeng, J.-K.; Zhang, C.-X. Research on the transmission loss of the floor aluminum profile for the high-speed train based on FE-SEA hybrid method. *J. Vibroengineering* **2016**, *18*, 1968–1981. [\[CrossRef\]](#)
- Deng, T.-S.; Sheng, X.-Z.; Jeong, H.; Thompson, D.-J. A two-and-half dimensional finite element/boundary element model for predicting the vibro-acoustic behaviour of panels with poro-elastic media. *J. Sound Vib.* **2021**, *505*, 116147. [\[CrossRef\]](#)
- Yao, D.; Zhang, J.; Wang, R.-Q.; Xiao, X.-B. Vibroacoustic damping optimisation of high-speed train floor panels in low- and mid-frequency range. *Appl. Acoust.* **2020**, *174*, 107788. [\[CrossRef\]](#)
- Wang, R.-Q.; Yao, D.; Zhang, J.; Xiao, X.-B.; Jin, X.-S. Effect of the laying order of core layer materials on the sound-insulation performance of high-speed train carbody. *Materials* **2023**, *16*, 3862. [\[CrossRef\]](#)
- Kim, H.; Ryue, J.; Thompson, D.-J.; Müller, A.-D. Application of a wavenumber domain numerical method to the prediction of the radiation efficiency and sound transmission of complex extruded panels. *J. Sound Vib.* **2019**, *449*, 98–120. [\[CrossRef\]](#)
- Kotsiantis, S.-B.; Zaharakis, I.-D.; Pintelas, P.-E. Machine learning: A review of classification and combining techniques. *Artif. Intell. Rev.* **2006**, *26*, 159–190. [\[CrossRef\]](#)
- Ahmad, Z.; Nguyen, T.-K.; Ahmad, S.; Nguyen, C.-D.; Kim, J.-M. Multistage centrifugal pump fault diagnosis using informative ratio principal component analysis. *Sensors* **2022**, *22*, 179. [\[CrossRef\]](#) [\[PubMed\]](#)
- Rahman, A.-P.; Putra, A.-A.; Ekojono; Apriyani, M.-E.; Rahmanto, A.-N.; Ghoneim, S.-S.; Mahmoud, K.; Lehtonen, M.; Darwish, M.-M. Precise transformer fault diagnosis via random forest model enhanced by synthetic minority over-sampling technique. *Electr. Power Syst. Res.* **2023**, *220*, 109361. [\[CrossRef\]](#)
- Zhou, Z.; Wen, C.-L.; Yang, C.-J. Fault isolation based on k-nearest neighbor rule for industrial processes. *IEEE Trans. Ind. Electron.* **2016**, *63*, 2578–2586. [\[CrossRef\]](#)
- Casaburo, A.; Magliacano, D.; Petrone, G.; Franco, F.; Rosa, S.-D. Gaussian-based machine learning algorithm for the design and characterization of a porous meta-material for acoustic applications. *Appl. Sci.* **2022**, *12*, 333. [\[CrossRef\]](#)
- Bader, E.-M.; Ménard, S.; Bard, H.-D.; Kouyoumji, J.-L.; Vardaxis, N.-G. Prediction of sound insulation using artificial neural networks—Part I: Lightweight wooden floor structures. *Acoustics* **2022**, *4*, 203–226. [\[CrossRef\]](#)
- Aloisio, A.; Rosso, M.-M.; De Leo, A.-M.; Fragiaco, M. Damage classification after the 2009 L'Aquila earthquake using multinomial logistic regression and neural networks. *Int. J. Disaster Risk Reduct.* **2023**, *96*, 103959. [\[CrossRef\]](#)

19. Malekjafarian, A.; Sarrabezolles, C.-A.; Khan, M.-A.; Golpayegani, F. A machine-learning-based approach for railway track monitoring using acceleration measured on an in-service train. *Sensors* **2023**, *23*, 7568. [[CrossRef](#)]
20. *ISO 10140-2:2021*; Acoustics—Laboratory Measurement of Sound Insulation of Building Elements—Part 2: Measurement of Airborne Sound Insulation. International Organization for Standardization: Geneva, Switzerland, 2021.
21. *ISO 717-1:2013*; Acoustics—Rating of Sound Insulation in Buildings and of Building Elements—Part 1: Airborne Sound Insulation. International Organization for Standardization: Geneva, Switzerland, 2013.
22. *ASTM C423-09a*; Standard Test Method for Sound Absorption and Sound Absorption Coefficients by the Reverberation Room Method. ASTM International: West Conshohocken, PA, USA, 2009.
23. Breiman, L. Random forests. *Mach. Learn.* **2001**, *45*, 5–32. [[CrossRef](#)]
24. Sun, X.-R.; Chai, J. Random forest feature selection for partial label learning. *Neurocomputing* **2023**, *561*, 126870. [[CrossRef](#)]
25. Janitza, S.; Celik, E.; Boulesteix, A.-L. A computationally fast variable importance test for random forests for high-dimensional data. *Adv. Data Anal. Classif.* **2018**, *12*, 85–915. [[CrossRef](#)]
26. Epifanio, I. Intervention in prediction measure: A new approach to assessing variable importance for random forests. *BMC Bioinform.* **2017**, *18*, 230. [[CrossRef](#)] [[PubMed](#)]
27. Liu, S.-M.; Huang, Z.-W.; Zhu, J.-M.; Lin, B.-L. Continuous blood pressure monitoring using photoplethysmography and electrocardiogram signals by random forest feature selection and GWO-GBRT prediction model. *Biomed. Signal Process. Control* **2023**, *88*, 105354. [[CrossRef](#)]
28. Hua, L.; Zhang, C.; Sun, W.; Li, Y.-M.; Xiong, J.-L.; Muhammad, S.-N. An evolutionary deep learning soft sensor model based on random forest feature selection technique for penicillin fermentation process. *ISA Trans.* **2023**, *136*, 139–151. [[CrossRef](#)]
29. Hardy, A.-E. Railway passengers and noise. *Proc. Inst. Mech. Eng. Part F J. Rail Rapid Transit* **1999**, *213*, 173–180. [[CrossRef](#)]
30. Thompson, D.-J.; Iglesias, E.-L.; Liu, X.-W.; Zhu, J.-Y.; Hu, Z.-W. Recent developments in the prediction and control of aerodynamic noise from high-speed trains. *Int. J. Rail Transp.* **2015**, *3*, 119–150. [[CrossRef](#)]

**Disclaimer/Publisher’s Note:** The statements, opinions and data contained in all publications are solely those of the individual author(s) and contributor(s) and not of MDPI and/or the editor(s). MDPI and/or the editor(s) disclaim responsibility for any injury to people or property resulting from any ideas, methods, instructions or products referred to in the content.